Carbon and hydrogen isotope fractionation of phthalate esters during degradation by sulfate and hydroxyl radicals

Dan Zhang[1,2], Langping Wu[2], Jun Yao[3**], Hartmut Herrmann[4], Hans-Hermann Richnow[2,3*]

[1]School of Energy and Environmental Engineering, University of Science and Technology Beijing, Xueyuan Road No.30, Haidian District, Beijing 100083, PR China

[2]Department of Isotope Biogeochemistry, Helmholtz Centre for Environmental Research-UFZ, Permoserstraße 15, Leipzig 04318, Germany

[3]School of Water Resources and Environment, China University of Geosciences (Beijing), Xueyuan Road No.29, Haidian District, Beijing 100083, PR China

[4]Atmospheric Chemistry Department (ACD), Leibniz Institute for Tropospheric Research (TROPOS), Permoserstraße 15, Leipzig 04318, Germany

* To whom correspondence should be addressed

* hans.richnow@ufz.de Tel.: +49 (0) 341 235 1212, Fax: +49 (0) 341 235 1443

** yaojun@cugb.edu.cn Tel.: +86 (0)10 82321958, Fax: +86 (0)10 82321958

ABSTRACT

This study investigated ^{13}C and ^{2}H isotope fractionation associated with oxidation of three phthalate esters (PAEs) by radical species, including sulfate radical ($SO_4^{\cdot-}$) induced by heat-activated persulfate (PS) and hydroxyl radical (HO·) induced by UV/H_2O_2. For persulfate oxidation at pH = 2 and pH = 7, similar carbon isotope fractionation (ε_C) but distinct hydrogen isotope enrichment factors (ε_H) were observed. The UV/H_2O_2 reaction of three PAEs showed smaller ε_H values in comparison with persulfate oxidation. The correlation of ^{2}H and ^{13}C fractionation (Λ) allows to distinguish the persulfate oxidation (25.7±2.6) and UV/H_2O_2 oxidation (2.4±0.2) of diethyl phthalate (DEP) highlighting the potential of compound-specific stable isotope analysis (CSIA) to characterize chemical oxidation mechanism of PAEs. Moreover, study of radical quenching and CSIA were combined to explore the dominant radical species during persulfate oxidation of DEP. $SO_4^{\cdot-}$ was found to be the predominant radical at pH = 2. Both $SO_4^{\cdot-}$ and HO· contributed to DEP degradation at pH = 7 and HO· was estimated to have a contribution of 21-63% according to dual C-H isotope fractionation values. Carbon and hydrogen apparent kinetic isotope effects (AKIEs) (^{13}C-AKIE =1.017, ^{2}H-AKIE =2.41) obtained from dominating sulfate radical reaction of DEP both supported the hypothesis of C-H bond cleavage. Thus, carbon and hydrogen isotope enrichment factors clearly distinguish the different reaction mechanisms and hence, are a promising approach to improve understanding of radical species reaction pathways for chemical oxidation of PAEs.

Keywords: Compound-specific stable isotope analysis; Phthalate esters; Isotope fractionation; Sulfate radical; Hydroxyl radical

1. Introduction

Phthalate esters (PAEs) are widely used as plasticizers and additives in numerous products, such as polyvinylchloride (PVC), cosmetics, medical devices, plastic toys and detergents . Worldwide production of PAEs is more than 8 million tons per year . PAEs are not linked by covalent bonds within the product matrix. Therefore, they can be leached out from the matrix e.g. by organic solvents or by diffusion . Previous studies reported contamination of PAEs in environmental compartments such as atmosphere (in and out door air, aerosols), water, sediment, soil, tissues and fluids of wildlife and humans. Consequently, PAEs have caused increasing concerns due to the potential hepatotoxic, teratogenic and carcinogenic effects . Dimethyl phthalate (DMP), diethyl phthalate (DEP) and dibutyl phthalate (DBP) have been listed as priority pollutants by US Environmental Protection Agency (EPA) . Several other environmental agencies from the European Union, China and Canada either classify some commonly occurring PAEs as priority pollutants or limit their use in children's toys . Therefore, knowledge about the different degradation processes is needed for efficient and economic removal of PAEs in the environment.

In situ chemical oxidation (ISCO) has become a promising technique for the removal of organic contaminants in soil, groundwater and aquifers making use of radical oxidation reactions . Hydrogen peroxide (H_2O_2) and persulfate (PS) are widely used oxidants in ISCO . UV/H_2O_2 is an efficient approach to produce hydroxyl radicals (HO·) and has been used to degrade organic compounds such as PAEs, BPA, dyes, benzene and PAHs . Over the last few years, sulfate radicals ($SO_4^{\cdot-}$) generated by PS or peroxymonosulfate (PMS) are considered as an alternative to HO· due to its long lifetime and high redox potential . Heat-activation is a commonly used activation method and it becomes attractive when combined with in situ thermal remediation . It has been reported that $SO_4^{\cdot-}$ is able to oxidize a variety of compounds, including

70PAEs, BTEX, PCBs, PAHs etc. . Meanwhile it is well demonstrated that the formation
71of $SO_4^{\cdot-}$ and HO· is pH dependent in activated PS system . Radical quenching studies
72are mainly used to distinguish dominant radical species according to different
73reactivities to probe potential radicals and their reaction with compounds. However, it
74is still not clear how to quantify the relative contribution of $SO_4^{\cdot-}$ and HO·. Only few
75studies calculated the relative contribution of $SO_4^{\cdot-}$ and HO· to the oxidation reaction
76based on different transformation yields or rate constants . Hence, it would be
77important to explore other possible ways on radical contribution estimation in order to
78investigate the complex interaction of radicals with PAEs and utilize the full potential
79of ISCO processes.

80 Compound-specific stable isotope analysis (CSIA) has received increasing
81attention in monitoring the fate of organic contaminants based on isotope fractionation
82concepts . CSIA has been successfully applied to identify sources, assess natural
83attenuation of contaminants and investigate reaction mechanisms on both chemical
84reaction and biodegradation in contaminant hydrology and organic (bio)-geochemistry
85. In the last decades, several studies showed the potential of multi-element CSIA
86($\delta^{13}C$, $\delta^{2}H$, $\delta^{37}Cl$, $\delta^{15}N$ etc.) to explore different transformation processes . For
87example, dual element stable isotope analysis of $\delta^{13}C$ and $\delta^{2}H$ was found sensitive to
88analyze sites of C-H bond cleavage (ring vs side chain) during oxidation of substituted
89benzenes . In previous studies, the application of CSIA on PAEs mainly focused on
90the carbon isotope fractionation during photolysis and biodegradation . To our best
91knowledge, studies on multi-element CSIA during PS oxidation and UV/H_2O_2 have
92not yet been reported for PAEs. This knowledge is essential for the application of
93stable isotope techniques to identify and quantify the removal of PAEs by advanced
94oxidation processes in remediation applications.

95 The main objectives of this study were (i) to investigate the potential of ^{13}C and ^{2}H

96isotope analysis for characterizing different oxidation processes (heat-activated PS 97oxidation and UV/H_2O_2) of three PAEs, (ii) to estimate the role of $SO_4^{\cdot-}$ and HO· 98during DEP oxidation and (iii) to explore apparent kinetic isotope effects (AKIEs) of 99two radicals' reaction with DEP. Isotope enrichment factors of ε_C and ε_H for all 100reactions were determined. A combined method based on radical quenching and CSIA 101was established to identify potential radical species which are responsible for the 102degradation of DEP. Moreover, extended Rayleigh-type equations and 2D-CSIA were 103used for the first time to estimate the relative contribution of $SO_4^{\cdot-}$ and HO· induced 104degradation of DEP. The reported ^2H and ^{13}C fractionation factors have the potential to 105be a reference for characterizing different degradation processes in environmental 106studies.

107**2. Materials and methods**

108*2.1. Chemicals*

109 DMP, DEP and DBP with 99.5% purity (analytical grade) were purchased 110from Sinopharm Chemical Reagent Co., Ltd. (Shanghai, China) and used without 111further purification. Potassium persulfate ($K_2S_2O_8$), hydrogen peroxide (30% H_2O_2), 112naphthalene (99%), di-potassium hydrogen phosphate (K_2HPO_4) and potassium 113dihydrogen phosphate (KH_2PO_4) were obtained from Merck (Guaranteed reagent 114quality, Darmstadt, Germany). Hydrochloric acid solution (HCl, 6 mol L^{-1}), hexane 115and ethanol were supplied by Carl Roth GmbH + Co. KG (Karlsruhe, Germany). 116Ortho-xylene and *tert*-butyl alcohol (TBA, 99.5%) were purchased from Sigma-117Aldrich (Munich, Germany). Sulfuric acid (25%, w/w), acetone, acetonitrile and 118dichloromethane (DCM) were supplied by Chem solute, Th. Geyer (Germany). 119Deionized water was produced by a Milli-Q system (>18.2 MΩ cm^{-1}, Millipore 120GmbH, Schwalbach/Ts. Germany) and used to prepare all experimental solutions.

121*2.2. Experimental procedures*

122*2.2.1. Heat-activated persulfate oxidation*

123 Persulfate oxidation reactions were conducted as batch experiments in a series of 124glass vials. A phosphate buffer solution was used to keep pH values stable and to 125maintain degradation condition constant during the whole reaction . Potassium 126persulfate ($K_2S_2O_8$) was used to generate $SO_4^{\cdot-}$ at pH = 2 and pH = 7. The pH value 127was adjusted by sulfuric acid (25% H_2SO_4). Preliminary experiment with persulfate at 128pH =10 showed the degradation kinetic of DEP was similar to the one obtained for 129alkaline hydrolysis at the same pH (data not shown), thus we do not further analyze 130persulfate oxidation at alkaline pH. An activation temperature of 35 °C was chosen for 131persulfate oxidation. Initial concentrations of PAEs were 1.09 mM DMP, 0.97 mM 132DEP and 0.037 mM DBP, respectively, considering different solubilities in water and 133to achieve adequate signal intensity for isotope measurements. The molar ratio of 134persulfate and PAEs was 50:1. Control experiments were conducted without addition 135of persulfate under identical conditions simultaneously. At different time intervals, 136reaction vials were removed and three PAEs were extracted by liquid-liquid 137extraction. 2 mL of DCM containing 500 mg L^{-1} ortho-xylene (as internal standard) 138was added to extract DMP and DEP from the aqueous solution. For DBP, 1 mL of 139hexane containing 100 mg L^{-1} naphthalene (as internal standard) was used as solvent 140in order to obtain good extraction efficiency.

141 To investigate the roles of $SO_4^{\cdot-}$ and HO· species formed in PS oxidation at pH = 1422 and pH = 7, radical quenching experiments were carried out separately in the 143presence of ethanol (EtOH) and *tert*-butyl alcohol (TBA). The radical scavengers 144(EtOH and TBA) were added to obtain a concentration of 195 mM, which 145corresponded to a 200:1 molar ratio of the radical scavengers compared to target 146compound (DEP). The second order rate constant of HO· with TBA ($k_{TBA/HO\cdot} = 6\times10^8$ 147$M^{-1}s^{-1}$) is almost 3 orders of magnitude faster than that of $SO_4^{\cdot-}$ with TBA ($k_{TBA/SO4\cdot-}$ =

1484×10^5 $M^{-1}s^{-1}$) . TBA was always used as a chemical probe to quench HO· completely 149but $SO_4^{\cdot-}$ partially and thus differentiate these two radicals. EtOH was considered to 150quench $SO_4^{\cdot-}$ and HO· simultaneously .

151*2.2.2. UV/H_2O_2 photolysis*

152 The reactions of three PAEs in UV/H_2O_2 system were carried out as the 153representative experiment of HO· dominant reactions. The photodegradation system 154consisted of a 200-mL Pyrex cylindrical flask with quartz window and was equipped 155with a 150 W xenon lamp (Hamamatsu, Japan). The xenon lamp covered a broad 156continuous spectrum from 185 nm to 2000 nm. A filter was used to cut off 157wavelengths shorter than 280 nm and to avoid reactions in this range. DEP in water 158showed no significant UV absorption at wavelengths longer than 280 nm, suggesting 159the absence of direct photolysis when a filter was used (Figure S2). The reaction 160solution consisted of 200 mL phosphate buffer solution at pH = 7. Initial 161concentrations of PAEs were the same as those in PS oxidation experiments. HO· 162radicals were generated by adding 30% H_2O_2, producing a molar ratio of 30:1 between 163H_2O_2 and PAEs. The experiment was carried out at 20±1 °C using a temperature-164controlled cooling system. The reaction solution was mixed with a magnetic stirrer at 165250 rmp throughout the whole experiment. At different time intervals, aliquots of the 166reaction solution were withdrawn using a syringe and extracted by liquid-liquid 167extraction as described in Section 2.2.1.

168*2.3. Concentration and isotope analysis*

169*2.3.1. GC-FID and GC-MS analysis*

170 Gas chromatography (7820A, Agilent, USA) coupled with flame ionization 171detection (GC-FID) was applied to determine the concentration of PAEs (DMP, DEP 172and DBP). A HP-5 column (30 m× 0.32 mm i.d., 0.25 μm, Agilent, USA) was used to 173separate compounds. The oven temperature program was 60 °C (held 2 min) followed

174by a ramp of 10 °C min^{-1} to 290 °C (held 2 min). The carrier gas was helium (1.5 mL 175min^{-1}). Samples were injected in split mode with a split ratio of 30:1 (1 μL) and the 176injector temperature was set at 250 °C. An Agilent GC-MS (7890A-5975C) system 177with the same column and GC parameters was used to identify potential degradation 178products.

179*2.3.2. Carbon and hydrogen isotope analysis*

180 Carbon and hydrogen isotope compositions of PAEs were measured by gas 181chromatography-isotope ratio mass spectrometry (GC-IRMS, MAT 253, Thermo-182Finnigan, Germany). Samples were injected in split mode (5:1, 1 μL) for carbon 183isotope measurement, and splitless mode was used for hydrogen isotope analysis to 184obtain optimum signal intensity. Good separation and peak shape of analytes were 185achieved using a ZB-1 column (60 m× 0.32 mm i.d., 1 μm, Phenomenex Inc., USA). 186The GC oven temperature program and other GC parameters were the same as those 187used for the GC-FID (see above). Reproducibility of $\delta^{13}C$ and $\delta^{2}H$ values was 188monitored by triplicate injections for each sample. The uncertainties of all samples 189were within typical analytical uncertainties ($\delta^{13}C$: ±0.5‰, $\delta^{2}H$: ±5‰).

190*2.4. Data evaluation*

191*2.4.1. Evaluation of isotope fractionation*

192 Carbon and hydrogen isotope fractionation of PAEs during chemical reactions 193were evaluated using the Rayleigh equation which is expressed as follows :

194 $$\ln\frac{\delta_t+1}{\delta_0+1}=\varepsilon\times\ln f \qquad (1)$$

195where δ_t and δ_0 are the isotope compositions of substrate at time t and zero, f is the 196remaining fraction of substrate at time t ($f = C_t/C_0$), and ε is obtained as the bulk 197isotope enrichment factor. For the correlation of ^{2}H and ^{13}C isotope values the isotopic 198shifts of hydrogen ($\delta^{2}H$) and carbon ($\delta^{13}C$) were presented as $\Delta\delta^{2}H$ vs $\Delta\delta^{13}C$ during

199degradation process. A linear regression of $\Delta\delta^2H$ and $\Delta\delta^{13}C$ was used to calculate the 200slope (Λ) for the relationship between hydrogen and carbon isotope fractionation.

201*2.4.2. Extended Rayleigh-type equations*

202 An extended Rayleigh-type equation (Equation 2) was derived to calculate the 203contribution of two processes degrading the same substrate simultaneously by two 204different mechanisms . *F* is the rate ratio of the first process to the overall reaction 205where two competing degradation pathways occurred, ε_A, ε_1 and ε_2 are the kinetic 206isotope enrichment factors of the overall reaction, the individual process 1 and 2, 207respectively.

208 $$F = \frac{\varepsilon_A - \varepsilon_2}{\varepsilon_1 - \varepsilon_2} \qquad (2)$$

209 For improved two-dimensional isotope analysis, dual element stable isotope data 210was used in a modified version of the Rayleigh equation to estimate the individual 211contributions of two competing pathways to the overall degradation. The rate ratio *F* 212is obtained as

213 $$F = \frac{\wedge \varepsilon_{C_2} - \varepsilon_{H_2}}{(\varepsilon_{H_1} - \varepsilon_{H_2}) - \wedge(\varepsilon_{C_1} - \varepsilon_{C_2})} \qquad (3)$$

214where Λ is the relationship of isotope shifts of two isotope pairs (H-C), and the ε 215values are the corresponding isotope enrichment factors associated with two 216individual processes.

217*2.4.3. Apparent kinetic isotope effect (AKIE) calculation*

218 For the Rayleigh equation, ε values are calculated from compound-average 219isotope data whereas the intrinsic isotope effect is position specific associated with the 220reaction step . Therefore, in order to investigate underlying reaction mechanisms and 221degradation pathways, it is crucial to convert observable ε values into AKIEs.

222Equation 4 is used to correct bulk isotope enrichment factors for isotopic dilution, the 223number of reactive sites within the molecule, as well as intra-molecular isotopic 224competition .

225 $$\mathrm{AKIE} = \frac{1}{1+\frac{n}{x} z \cdot \varepsilon_{\mathrm{bulk}}\ (‰)/1000} \qquad (4)$$

226where ε_{bulk} is the bulk isotope enrichment factor, n is the number of atoms of the 227element considered in the molecule, x is the number of atoms at reactive positions and 228z is the number of indistinguishable reactive positions.

229**3. Results and discussion**

230*3.1. Degradation kinetics of PAEs*

231 Three PAEs (DMP, DEP and DBP) with different lengths of alkyl side chain were 232selected in this study. The chemical oxidation processes of three PAEs followed 233pseudo-first order kinetics in all experiments ($R^2 \geq 0.965$, Table 1). Control 234experiments of DEP by direct UV radiation, UV radiation with filter and hydrolysis at 23535 °C showed negligible degradation compared to chemical oxidation (Fig. S1, S2). 236Rate constants (k) for the UV/H_2O_2 reaction of DMP (0.0528 h^{-1}), DEP (0.0541 h^{-1}) 237and DBP (0.1115 h^{-1}) were determined to describe the reaction (Table 1). A previous 238study showed that the calculated k values increased with the number of carbon atom 239in the alkyl side chain of PAEs during ·OH-initiated photodegradation using 240transition-state theory. The activation energies for the reaction of the three PAEs differ 241with the chemical structure and the rate constants of the PAEs degradation due to 242UV/H_2O_2 reaction are probably related to the ·OH reaction with the aromatic ring and 243the side chain. During persulfate oxidation of PAEs, the temperature was chosen at 35 244°C for milder reaction condition. The pH value is considered to be an important factor 245for reaction kinetics and radical species, therefore the removal of three PAEs by

246persulfate oxidation was studied at pH = 2 and pH = 7. Three PAEs presented
247different degradation kinetic behaviors. For DEP and DBP, rate constants at pH = 2
248are larger than those at pH = 7, which is consistent with previous results of Li et al.
249indicating that acidic condition had positive effect on DBP degradation due to the
250predominant radical species of $SO_4^{\cdot-}$. However, DMP seems to show a different
251kinetic trend, resulting in a slightly smaller removal rate at pH = 2. Wang et al.
252reported similar rate constants of DMP at pH = 3.1 and pH = 7.0 by thermally
253activated persulfate oxidation, which indicated that initial pH values had a minor
254effect on the rate constants of DMP. The different reaction kinetic of DMP compared
255to DEP and DBP could be probably related to different dominant radical species and
256their affinity to react with the longer alkyl side chain of the PAE molecules.

257*3.2. Carbon and hydrogen isotope fractionation patterns of PAEs during chemical*
258*oxidation*

259 Both carbon and hydrogen isotopic values of three PAEs from all investigated
260reactions showed the trend to more positive values during the degradation, which
261indicates a normal isotope effect (Fig. S3). The carbon and hydrogen isotope
262enrichment factors of DMP, DEP and DBP can be quantified using Rayleigh equation
263(Fig. 1). The Rayleigh regression of all three PAEs exhibited high correlation
264coefficients ($R^2 \geq 0.960$) for δ^2H and $\delta^{13}C$ and the uncertainty was within the 95%
265confidence interval (C.I.) (Table 1). For the UV/H_2O_2 reaction, carbon isotope
266enrichment factors (ε_C) of DMP, DEP and DBP ranged from -2.76±0.25‰, to
267-2.30±0.42‰, to -0.92±0.16‰, respectively. ε_C values decreases with increasing
268length of the alkyl side chain in the PAE molecules. This result is likely related to the
269isotope dilution effect caused by carbon atoms in non-reactive positions . During heat-
270activated persulfate oxidation, as shown in Table 1, degradation rate constants of three
271PAEs vary at pH = 2 and pH = 7. However, ε_C values remain similar for each PAE

272compared to those obtained from the UV/H_2O_2 reaction. The isotope dilution effect is
273also observed for DMP, DEP and DBP. Therefore, carbon isotope fractionation
274patterns alone are not sufficient to distinguish between UV/H_2O_2 and PS oxidation
275processes. In contrast, ε_H values obtained from the degradation of three PAEs in the
276UV/H_2O_2 reaction are much smaller than those from PS oxidation. Furthermore, for
277reaction with heat-activated PS oxidation, ε_H values range from -8.7±1.2‰ (pH = 7)
278to -23.9±2.4‰ (pH = 2) for DMP, from -28.3±3.3‰ (pH = 7) to -41.8±2.4‰ (pH = 2)
279for DEP and from -24.6±1.8‰ (pH = 7) to -31.0±2.0‰ (pH = 2) for DBP. In this case,
280δ^2H values of three PAEs show a similar trend to a larger hydrogen isotope
281fractionation at pH = 2 compared to pH = 7. Thus, distinctly different hydrogen
282enrichment factors could be used to distinguish different reaction processes. The
283increase of ^{2}H fractionation might be an indication that $SO_4^{\cdot-}$ radicals become a major
284species at low pH in persulfate oxidation reactions leading to larger hydrogen isotope
285fractionation compared to high pH where $SO_4^{\cdot-}$ and HO· coexist (see discussion
286below). Contrary to the carbon isotope fractionation pattern, ε_H values of DMP, DEP
287and DBP do not show a consistent trend for an isotope dilution effect with increasing
288length of the alkyl side chain during PS oxidation experiments. This is due to the
289possibility that different dominant pathways are responsible for the decomposition of
290three PAEs with different alkyl side chain lengths, as suggested in a previous
291computational study on HO·-initiated photochemical transformation of four PAEs .

292*3.3. Correlation of ^{2}H and ^{13}C isotope fractionation to differentiate reaction processes*

293 The correlation of hydrogen and carbon isotopic values of three PAEs undergoing
294different reactions was compared individually in dual isotope plots. All investigated
295experiments showed a well-fitted linear correlation (Fig. 2). For reaction with
296UV/H_2O_2 and PS oxidation of DMP, different slopes ($\Lambda = \Delta\delta^2H/\Delta\delta^{13}C$) are observed
297ranging from 2.0±0.1 to 13.1±1.4 (Table 1), which is attributable to different ε_H values

298(ranging from -4.8±0.5‰ to -23.9±2.4‰) and similar ε_C values (ranging from 299-2.08±0.10‰ to -2.76±0.25‰). Similarly, significant variations of Λ values (2.4±0.2, 30014.9±3.0 and 25.7±2.6) are obtained for DEP during three reactions. In this case, 301distinct dual H-C isotope slopes of DMP and DEP for radical oxidation processes 302open the possibility of 2D-CSIA to differentiate chemical oxidation reactions of PAEs 303in the field. However, DBP showed a different trend with almost identical Λ values at 304pH = 2 (39.0±3.4) and pH = 7 (35.3±4.5) during persulfate oxidation. Despite this, the 305correlation of ^{2}H and ^{13}C isotope fractionation obtained for DBP also could be used to 306distinguish between UV/H_2O_2 (9.0±2.3) and persulfate oxidation reaction. Even if 307distinct ε_H values have the potential to distinguish reactions, the dual element isotope 308approach may be recommended for field studies. A significant advantage is that 309possible transport and retardation processes on the extent of isotope fractionation can 310be canceled out because they may have a similar influence on both elements . The 311difference between dual element isotope fractionation patterns of UV/H_2O_2 and PS 312oxidation could be due to distinct dominant radical species leading to the degradation 313of PAEs. In addition, significant isotope discrimination of DMP and DEP for PS 314oxidation at pH = 2 and pH = 7 is likely associated with different radical species. 315Interestingly, the similar Λ values at pH = 2 and pH = 7 for DBP were not observed 316for DMP and DEP, which might be partly explained with the influence of the chemical 317structure, particularly the alkyl side chain which is a potential target for radicals. It is 318conceivable that the competing reactions at the side chain and aromatic rings are 319changing with chain length but we cannot quantify the reaction to prove this 320hypothesis. Therefore, more research is needed to understand the precise mechanisms 321of free radical reactions with the alkyl side chain of PAEs and which affect the Λ 322values.

323*3.4. Identification of predominant radical species by studying radical quenching*

combined with CSIA

Previous studies have demonstrated that $SO_4^{\cdot-}$ and HO· were probably generated and responsible for the decomposition of organic contaminants in persulfate oxidation system . Predominant radical species during heat-activated PS oxidation were investigated using two alcoholic radical scavengers. EtOH and TBA were added to the solution, respectively and corresponded to a 200:1 molar ratio of the radical scavengers and DEP. Both $SO_4^{\cdot-}$ and HO· could be quenched by EtOH due to the second-order rate constants of 1.2-2.8×10^9 $M^{-1}s^{-1}$ for EtOH/HO· system and 1.6-7.7×10^7 $M^{-1}s^{-1}$ for EtOH/$SO_4^{\cdot-}$ system . TBA is considered as an efficient scavenger of HO·, because TBA reacts relatively slowly with $SO_4^{\cdot-}$ (k= 4-9.1×10^5 $M^{-1}s^{-1}$) compared to high reactivity of TBA/HO· system (k= 3.8-7.6×10^8 $M^{-1}s^{-1}$) . After the addition of EtOH, the removal of DEP by persulfate could be neglected compared to experiments without scavenger at pH = 2 and pH = 7 (Fig. 3), which indicates that PS oxidation processes are mostly attributed to free radical reactions of $SO_4^{\cdot-}$ and HO·. In the presence of TBA, strong inhibiting effects on the degradation of DEP were observed. A slightly smaller degree of inhibition than that of EtOH possibly indicates the presence of $SO_4^{\cdot-}$ during PS oxidation of DEP. However, results for degradation kinetics of radical quenching experiments in this study are not sufficient to identify dominant radical species at pH = 2 and pH = 7 due to strong inhibition of EtOH and TBA. In order to explore predominant reactive species responsible for the degradation of DEP, carbon and hydrogen isotope fractionations of TBA quenching experiments were investigated. Contrary to the distinct ε_H and Λ values of PS oxidation with DEP at pH = 2 and pH = 7, the obtained ε_H and Λ values after the addition of TBA were very similar (Table 1, Fig. 2). The difference between PS oxidation and TBA quenching experiments could be due to different radical species contributing to the overall reaction. In the presence of TBA, $SO_4^{\cdot-}$ becomes the predominant radical

350species which is responsible for the degradation of DEP at pH = 2 and pH = 7 and
351which is consistent with isotope fractionation results. In addition, Λ values of DEP
352quenching experiments (Λ= 24.1±4.3 at pH = 7, Λ= 30.5±2.2 at pH = 2) are almost
353identical to that of PS oxidation at pH = 2 (Λ= 25.7±2.6). This result suggests that
354$SO_4^{\cdot-}$ is the dominant radical at pH = 2 during PS oxidation of DEP, while $SO_4^{\cdot-}$ as
355well as HO· probably contribute to the degradation at pH = 7 with a smaller Λ value
356of 14.9±3.0.

357*3.5. Estimating the relative contribution of $SO_4^{\cdot-}$ and HO· in the overall reaction*
358*using isotope fractionation analysis*

359 In previous studies , Rayleigh-type equations were modified to derive an equation
360for estimating the contribution of two simultaneous pathways to the overall
361degradation. To estimate the relative contribution of $SO_4^{\cdot-}$ and HO·, it is assumed that
362the impact of phosphate buffer on major radical species during PS oxidation is small.
363Phosphate buffer has been widely used to maintain a constant pH value in many
364studies due to low reactivity with sulfate and hydroxyl radicals . A phosphate buffer of
365up to 100 mM was used to keep the pH value constant. Still, the radical chain reaction
366with phosphate anions (HPO_4^{2-} and $H_2PO_4^-$) might affect the reaction. The potential
367formation of $HPO_4^{\cdot-}$ and $H_2PO_4^{\cdot}$ with respect to pH value and concentration of the
368phosphate buffer used in the experiments was estimated according to literature data
369(Excel SI). The potential contribution of phosphate radicals in the experiments of DEP
370was minor (<8%) and did not affect the discussion below (Text SI). Therefore, the
371contribution of secondary inorganic radical species was not considered further for the
372estimation of the relative contribution of $SO_4^{\cdot-}$ and HO·.

373 HO· is the predominant radical species in the UV/H_2O_2 reaction, whereas the
374TBA quenching experiment of DEP at pH = 7 suggests that $SO_4^{\cdot-}$ are the dominant
375radicals. In addition, distinct ^2H and ^{13}C isotope enrichment factors allow to estimate

376the relative contribution of $SO_4^{\cdot-}$ and HO· on the removal of DEP during PS oxidation 377at pH = 7 according to the extended Rayleigh-type equation. Error propagation was 378used to calculate the 95% confidence intervals of the estimated contribution (*F*) of 379HO· vs $SO_4^{\cdot-}$. HO· has a contribution of 0-47% and 20-50% based on the uncertainty 380of carbon and hydrogen isotope analyses, respectively. Moreover, Equation 3 was also 381applied to calculate the value of *F* using carbon and hydrogen isotope signatures 382simultaneously. A contribution of 21-63% for HO· was obtained, which is in 383agreement with hydrogen isotope result. The reason is that the reaction of DEP with 384$SO_4^{\cdot-}$/HO· shows similar carbon enrichment factors, but different hydrogen 385enrichment factors. In this case, it is recommended to estimate the relative 386contribution using hydrogen isotope data differently than data from carbon isotope 387analysis. Even though a wide range of variability is observed due to the uncertainty of 388Λ and ε values, preliminary results indicate that a combination of radical quenching 389experiments and CSIA has the potential to estimate the relative contribution of $SO_4^{\cdot-}$ 390and HO· in persulfate oxidation systems.

391*3.6. Apparent kinetic isotope effects of DEP with HO· and $SO_4^{\cdot-}$*

392 The intermediate products from DEP reaction with UV/H_2O_2 were investigated 393using GC-MS analysis. The main transformation product is tentatively identified as 394diethyl 3-hydroxyphthalate (Fig. S4) by the molecular ion, mass fragment peak and 395also by comparison with a previous study . HO· can oxidize organic compounds in 396aqueous media via three possible reaction mechanisms: (i) HO· addition leading to the 397radical adducts formation (RAF pathway), (ii) hydrogen atom transfer by HO· (HAT 398pathway) and (iii) single electron transfer by HO· (SET pathway) . Based on the 399identified transformation product, HO· addition to the aromatic ring of DEP is 400assumed to be the main reaction mechanism, which is consistent with Gauss 401computational results on HO·-initiated degradation of PAEs in a previous study . The

402values of $\delta^{13}C$ and $\delta^{2}H$ are measured as average isotope compositions in the 403compound, thus obtained ε_C and ε_H values are considered as bulk isotope fractionation 404factors. According to Equation 4, ε_C and ε_H can be converted into position specific 405apparent kinetic isotope effects (^{13}C-AKIE and ^{2}H-AKIE) considering the reactive 406sites and nonreactive positions in the molecule. Semi-classical Streitwieser Limit for 407kinetic isotope effects (KIE) of C-H bond cleavage are in the range of 1.01-1.03 for 408carbon isotopes and 2-8 for hydrogen isotopes . For calculation of ^{13}C-AKIE during 409UV/H_2O_2 reaction of DEP, the values of n, x and z are 12, 2 and 2, respectively. The 410calculated ^{13}C-AKIE of 1.028 falls in the range of 1.01-1.03 (Table 2), which supports 411the speculation of the RAF pathway. However, for ^{2}H, an AKIE of 1.11 was obtained, 412which is lower than the expected KIE_H of 2-8. Much smaller experimental kinetic 413isotope effects ($AKIE_H$) might be likely associated with a sp^2 to sp^3 hybridization 414change at the reacting carbon in the aromatic ring as reported elsewhere .

415 For the reaction of $SO_4^{\cdot-}$ with DEP, degradation products could not be identified 416by GC-MS analysis. The concentration of the metabolites was possibly very low and 417rapid degradation of metabolites in subsequent radical reaction may prevent detection 418of the products which would indicate hydroxylation of the side chain or the aromatic 419ring. Previous mechanistic studies on the reaction of sulfate radicals with PAEs 420suggested that the first step of $SO_4^{\cdot-}$ oxidation was likely the radical attack on the 421aromatic ring or oxidation of the aliphatic chain . Therefore, AKIEs were calculated 422for the reaction of DEP with $SO_4^{\cdot-}$ considering radical attack at the side chain and at 423the aromatic ring. In the presence of TBA, $SO_4^{\cdot-}$ becomes the predominant radical 424species responsible for DEP decomposition. ^{13}C-AKIE and ^{2}H-AKIE at pH = 2 were 4251.013 and 2.19, respectively, and considered to be identical for both pathways, 426because the number of reactive positions (x) and indistinguishable reactive positions 427(z) lead to calculation of identical AKIEs in this simplified approach (Equation 4).

Additionally, corresponding AKIEs for PS oxidation at pH = 2 and TBA quenching experiment at pH = 7 were shown in Table 2. As HO· and $SO_4^{\cdot-}$ radicals are both involved at pH = 7 during PS oxidation, it is difficult to confirm exact values of n, x and z for the radical reaction due to competing mechanisms. Therefore, ^{13}C-AKIE and ^{2}H-AKIE values are not calculated for PS oxidation at pH = 7 in this study. Although the obtained ^{13}C-AKIE and ^{2}H-AKIE values of $SO_4^{\cdot-}$ dominant reactions are both in accordance with expected KIE ranges for C-H bond oxidation (C:1.01-1.03, H: 2-8), it supports the hypothesis of C-H bond cleavage but cannot be used to predict degradation mechanisms at the side chain or aromatic ring of DEP with $SO_4^{\cdot-}$. More information on intermediate products may be needed for further elucidation of reaction mechanisms.

4. Conclusions

In present study, dual isotope fractionation of radical reactions was systematically investigated in heat-activated PS oxidation and UV/H_2O_2 for three PAEs (DMP, DEP and DBP). Distinct Λ values ($\Delta\delta^2H/\Delta\delta^{13}C$) indicate the potential of CSIA to characterize PS oxidation and UV/H_2O_2 reaction in field studies as an example for environmental remediation measures or technical systems. The combination of radical quenching analysis and CSIA suggests that $SO_4^{\cdot-}$ is the dominant radical species to oxidize DEP at pH = 2 during PS oxidation, while both $SO_4^{\cdot-}$ and HO· are the major species at pH = 7. Additionally, it provides a novel approach to estimate the relative contribution of $SO_4^{\cdot-}$ and HO· to the overall reaction using isotope fractionation for characterizing radical reactions. Carbon and hydrogen isotope fractionation patterns are of fundamental importance to evaluate ISCO processes for the removal of PAEs. The results of this study are an important step forward in understanding degradation mechanisms of organic compounds with $SO_4^{\cdot-}$ and HO· radicals in the aqueous phase.

Supplementary data

Further information about the remaining fraction of DEP in control experiments (Fig. S1), UV absorption spectrum of DEP in water (Fig. S2), carbon and hydrogen isotope compositions of PAEs (Fig. S3), mass spectrum of identified degradation product (Fig. S4) and the estimation of potential influence of phosphate buffer on radicals (Excel SI).

Acknowledgments

This work was supported by the China Scholarship Council (File No. 201506460058 for Dan Zhang, and File No. 201306460007 for Langping Wu) and in part by grants from the Key project from National Science Foundation of China (41430106). We are grateful to Steffen Kümmel for his help in the Isotope Laboratory of the UFZ.

References

[1] C.A. Staples, D.R. Peterson, T.F. Parkerton, W.J. Adams, The environmental fate of phthalate esters: A literature review, Chemosphere 35 (1997) 667-749.

[2] Y. Zhang, Q. Liang, R.T. Gao, H.B. Hou, W.B. Tan, X.S. He, H. Zhang, M.D. Yu, L. Ma, B.D. Xi, X.W. Wang, Contamination of phthalate esters (PAEs) in typical wastewater-irrigated agricultural soils in Hebei, North China, PLoS One 10 (2015) e0137998.

[3] C. Vamsee-Krishna, P.S. Phale, Bacterial degradation of phthalate isomers and their esters, Indian J. Microbiol. 48 (2008) 19-34.

[4] J.Q. Sun, X.Q. Wu, J. Gan, Uptake and metabolism of phthalate esters by edible plants, Environ. Sci. Technol. 49 (2015) 8471-8478.

[5] H. Chen, R. Zhuang, J. Yao, F. Wang, Y. Qian, A comparative study on the impact of phthalate esters on soil microbial activity, Bull. Environ. Contam. Toxicol. 91 (2013) 217-223.

[6] S. Net, R. Sempere, A. Delmont, A. Paluselli, B. Ouddane, Occurrence, fate, behavior and ecotoxicological state of phthalates in different environmental matrices, Environ. Sci. Technol. 49 (2015) 4019-4035.

[7] W.J. Tang, L.S. Zhang, Y. Fang, Y. Zhou, B.C. Ye, Biodegradation of phthalate esters by newly isolated *Rhizobium* sp. LMB-1 and its biochemical pathway of di-n-butyl phthalate, J. Appl. Microbiol. 121 (2016) 177-186.

[8] United States Environmental Protection Agency (USEPA), Electronic code of federal regulations, Title 40-Protection of environment, Appendix A to Part 423-126, Priority pollutants

488(2013).
489[9] D.W. Gao, Z.D. Wen, Phthalate esters in the environment: A critical review of their occurrence,
490biodegradation, and removal during wastewater treatment processes, Sci. Total Environ. 541
491(2016) 986-1001.
492[10] P. Devi, U. Das, A.K. Dalai, In-situ chemical oxidation: Principle and applications of
493peroxide and persulfate treatments in wastewater systems, Sci. Total Environ. 571 (2016) 643-657.
494[11] A. Tsitonaki, B. Petri, M. Crimi, H. MosbÆK, R.L. Siegrist, P.L. Bjerg, In situ chemical
495oxidation of contaminated soil and groundwater using persulfate: A review, Crit. Rev. Environ.
496Sci. Technol. 40 (2010) 55-91.
497[12] M. Cheng, G.M. Zeng, D.L. Huang, C. Lai, P. Xu, C. Zhang, Y. Liu, Hydroxyl radicals based
498advanced oxidation processes (AOPs) for remediation of soils contaminated with organic
499compounds: A review, Chem. Eng. J. 284 (2016) 582-598.
500[13] M. Gmurek, M. Olak-Kucharczyk, S. Ledakowicz, Photochemical decomposition of
501endocrine disrupting compounds - A review, Chem. Eng. J. 310 (2017) 437-456.
502[14] B. Xu, N.Y. Gao, X.F. Sun, S.J. Xia, M. Rui, M.O. Simonnot, C. Causserand, J.F. Zhao,
503Photochemical degradation of diethyl phthalate with UV/H_2O_2, J. Hazard. Mater. 139 (2007) 132-
504139.
505[15] B. Xu, N.Y. Gao, H. Cheng, S.J. Xia, M. Rui, D.D. Zhao, Oxidative degradation of dimethyl
506phthalate (DMP) by UV/H_2O_2 process, J. Hazard. Mater. 162 (2009) 954-959.
507[16] D.L. Huang, Y. Wang, C. Zhang, G.M. Zeng, C. Lai, J. Wan, L. Qin, Y. Zeng, Influence of
508morphological and chemical features of biochar on hydrogen peroxide activation: implications on
509sulfamethazine degradation, RSC Advances 6 (2016) 73186-73196.
510[17] D.L. Huang, C.J. Hu, G.M. Zeng, M. Cheng, P. Xu, X.M. Gong, R.Z. Wang, W.J. Xue,
511Combination of Fenton processes and biotreatment for wastewater treatment and soil remediation,
512Sci. Total Environ. 574 (2017) 1599-1610.
513[18] F. Ghanbari, M. Moradi, Application of peroxymonosulfate and its activation methods for
514degradation of environmental organic pollutants: Review, Chem. Eng. J. 310 (2017) 41-62.
515[19] Y.F. Ji, C.X. Dong, D.Y. Kong, J.H. Lu, Q.S. Zhou, Heat-activated persulfate oxidation of
516atrazine: Implications for remediation of groundwater contaminated by herbicides, Chem. Eng. J.
517263 (2015) 45-54.
518[20] X.L. Zhang, M.B. Feng, R.J. Qu, H. Liu, L.S. Wang, Z.Y. Wang, Catalytic degradation of
519diethyl phthalate in aqueous solution by persulfate activated with nano-scaled magnetic
520$CuFe_2O_4$/MWCNTs, Chem. Eng. J. 301 (2016) 1-11.
521[21] S. Wacławek, H.V. Lutze, K. Grübel, V.V.T. Padil, M. Černík, D.D. Dionysiou, Chemistry of
522persulfates in water and wastewater treatment: A review, Chem. Eng. J. 330 (2017) 44-62.
523[22] J.L. Wang, S.Z. Wang, Activation of persulfate (PS) and peroxymonosulfate (PMS) and
524application for the degradation of emerging contaminants, Chem. Eng. J. 334 (2018) 1502-1517.
525[23] A. Romero, A. Santos, F. Vicente, C. González, Diuron abatement using activated
526persulphate: Effect of pH, Fe(II) and oxidant dosage, Chem. Eng. J. 162 (2010) 257-265.
527[24] C.J. Liang, H.-W. Su, Identification of sulfate and hydroxyl radicals in thermally activated
528persulfate, Ind. Eng. Chem. Res. 48 (2009) 5558-5562.
529[25] G.P. Anipsitakis, D.D. Dionysiou, Radical Generation by the Interaction of Transition Metals
530with Common Oxidants, Environ. Sci. Technol. 38 (2004) 3705-3712.
531[26] S. Yuan, P. Liao, A.N. Alshawabkeh, Electrolytic manipulation of persulfate reactivity by iron

532electrodes for trichloroethylene degradation in groundwater, Environ. Sci. Technol. 48 (2014) 656-
533663.
534[27] M. Ahmad, A.L. Teel, O.S. Furman, J.I. Reed, R.J. Watts, Oxidative and reductive pathways
535in iron-ethylenediaminetetraacetic acid-activated persulfate systems, J. Environ. Eng. 138 (2012)
536411-418.
537[28] M. Elsner, G. Imfeld, Compound-specific isotope analysis (CSIA) of micropollutants in the
538environment-current developments and future challenges, Curr. Opin. Biotechnol. 41 (2016) 60-
53972.
540[29] M. Elsner, Stable isotope fractionation to investigate natural transformation mechanisms of
541organic contaminants: principles, prospects and limitations, J. Environ. Monit. 12 (2010) 2005-
5422031.
543[30] I. Nijenhuis, H.H. Richnow, Stable isotope fractionation concepts for characterizing
544biotransformation of organohalides, Curr. Opin. Biotechnol. 41 (2016) 108-113.
545[31] C. Vogt, C. Dorer, F. Musat, H.H. Richnow, Multi-element isotope fractionation concepts to
546characterize the biodegradation of hydrocarbons-from enzymes to the environment, Curr. Opin.
547Biotechnol. 41 (2016) 90-98.
548[32] N. Zhang, I. Geronimo, P. Paneth, J. Schindelka, T. Schaefer, H. Herrmann, C. Vogt, H.H.
549Richnow, Analyzing sites of OH radical attack (ring vs. side chain) in oxidation of substituted
550benzenes via dual stable isotope analysis ($\delta^{13}C$ and $\delta^{2}H$), Sci. Total Environ. 542 (2016) 484-494.
551[33] H. Liu, Z. Wu, X.Y. Huang, C. Yarnes, M.J. Li, L. Tong, Carbon isotopic fractionation during
552biodegradation of phthalate esters in anoxic condition, Chemosphere 138 (2015) 1021-1027.
553[34] X.W. Peng, X.G. Li, L.J. Feng, Behavior of stable carbon isotope of phthalate acid esters
554during photolysis under ultraviolet irradiation, Chemosphere 92 (2013) 1557-1562.
555[35] X.W. Peng, L.J. Feng, X.G. Li, Pathway of diethyl phthalate photolysis in sea-water
556determined by gas chromatography-mass spectrometry and compound-specific isotope analysis,
557Chemosphere 90 (2013) 220-226.
558[36] X.W. Peng, X.G. Li, Compound-specific isotope analysis for aerobic biodegradation of
559phthalate acid esters, Talanta 97 (2012) 445-449.
560[37] C.Q. Tan, N.Y. Gao, Y. Deng, Y.J. Zhang, M.H. Sui, J. Deng, S.Q. Zhou, Degradation of
561antipyrine by UV, UV/H_2O_2 and UV/PS, J. Hazard. Mater. 260 (2013) 1008-1016.
562[38] L.S. Lian, B. Yao, S.D. Hou, J.Y. Fang, S.W. Yan, W.H. Song, Kinetic study of hydroxyl and
563sulfate radical-mediated oxidation of pharmaceuticals in wastewater effluents, Environ. Sci.
564Technol. 51 (2017) 2954-2962.
565[39] Y. Yang, J. Jiang, X.L. Lu, J. Ma, Y.Z. Liu, Production of sulfate radical and hydroxyl radical
566by reaction of ozone with peroxymonosulfate: a novel advanced oxidation process, Environ. Sci.
567Technol. 49 (2015) 7330-7339.
568[40] P.C. Xie, J. Ma, W. Liu, J. Zou, S.Y. Yue, X.C. Li, M.R. Wiesner, J.y. Fang, Removal of 2-
569MIB and geosmin using UV/persulfate: contributions of hydroxyl and sulfate radicals, Water Res.
57069 (2015) 223-233.
571[41] B.M. van Breukelen, Extending the Rayleigh equation to allow competing isotope
572fractionating pathways to improve quantification of biodegradation, Environ. Sci. Technol. 41
573(2007) 4004-4010.
574[42] F. Centler, F. Hesse, M. Thullner, Estimating pathway-specific contributions to
575biodegradation in aquifers based on dual isotope analysis: theoretical analysis and reactive

transport simulations, J. Contam. Hydrol. 152 (2013) 97-116.
[43] C.M. Aelion, P. Höhener, D. Hunkeler, R. Aravena, Environmental isotopes in biodegradation and bioremediation, CRC Press (2009).
[44] M. Elsner, L. Zwank, D. Hunkeler, R.P. Schwarzenbach, A new concept linking observable stable isotope fractionation to transformation pathways of organic pollutants, Environ. Sci. Technol. 39 (2005) 6896-6916.
[45] Y. Gao, T. An, Y. Ji, G. Li, C. Zhao, Eco-toxicity and human estrogenic exposure risks from OH-initiated photochemical transformation of four phthalates in water: A computational study, Environ. Pollut. 206 (2015) 510-517.
[46] H. Li, J. Wan, Y. Ma, Y. Wang, Reaction pathway and oxidation mechanisms of dibutyl phthalate by persulfate activated with zero-valent iron, Sci. Total Environ. 562 (2016) 889-897.
[47] Z. Wang, D.Y. Deng, L.L. Yang, Degradation of dimethyl phthalate in solutions and soil slurries by persulfate at ambient temperature, J. Hazard. Mater. 271 (2014) 202-209.
[48] J. Palau, P. Jamin, A. Badin, N. Vanhecke, B. Haerens, S. Brouyere, D. Hunkeler, Use of dual carbon-chlorine isotope analysis to assess the degradation pathways of 1,1,1-trichloroethane in groundwater, Water Res. 92 (2016) 235-243.
[49] D.H. Han, J.Q. Wan, Y.W. Ma, Y. Wang, Y. Li, D.Y. Li, Z.Y. Guan, New insights into the role of organic chelating agents in Fe(II) activated persulfate processes, Chem. Eng. J. 269 (2015) 425-433.
[50] P. Neta, R.E. Huie, A.B. Ross, Rate constants for reactions of inorganic radicals in aqueous solution, J. Phys. Chem. Ref. Data 17 (1988) 1027-1284.
[51] C.J. Liang, Z.S. Wang, N. Mohanty, Influences of carbonate and chloride ions on persulfate oxidation of trichloroethylene at 20 °C, Sci. Total Environ. 370 (2006) 271-277.
[52] X.G. Gu, S.G. Lu, L. Li, Z.F. Qiu, Q. Sui, K.F. Lin, Q.S. Luo, Oxidation of 1,1,1-trichloroethane stimulated by thermally activated persulfate, Ind. Eng. Chem. Res. 50 (2011) 11029-11036.
[53] A. Ghauch, A.M. Tuqan, N. Kibbi, Ibuprofen removal by heated persulfate in aqueous solution: A kinetics study, Chem. Eng. J. 197 (2012) 483-492.
[54] K.S. Tay, N.A. Rahman, M.R. Bin Abas, Fenton degradation of dialkylphthalates: products and mechanism, Environ Chem Lett 9 (2011) 539-546.
[55] T. An, Y. Gao, G. Li, P.V. Kamat, J. Peller, M.V. Joyce, Kinetics and mechanism of $^{\bullet}OH$ mediated degradation of dimethyl phthalate in aqueous solution: experimental and theoretical studies, Environ. Sci. Technol. 48 (2014) 641-648.
[56] P.F. Cook, Enzyme mechanism from isotope effects, CRC Press (1991).
[57] L.J. Xu, W. Chu, L. Gan, Environmental application of graphene-based $CoFe_2O_4$ as an activator of peroxymonosulfate for the degradation of a plasticizer, Chem. Eng. J. 263 (2015) 435-443.

615

616**Table 1.** Degradation kinetic and isotope fractionation parameters of PAEs during chemical

617oxidation.

Conditions	k (h^{-1})	R^2	ε_C (‰)	R^2	ε_H (‰)	R^2	Λ	*f*
DMP_pH 2_PS	0.0024	0.986	-2.09±0.21[a]	0.994	-23.9±2.4	0.995	13.1±1.4	0.252
DMP_pH 7_PS	0.0037	0.983	-2.08±0.10	0.998	-8.7±1.2	0.985	4.8±0.5	0.055
DMP_pH 7_UV/H_2O_2	0.0528	0.980	-2.76±0.25	0.996	-4.8±0.5	0.994	2.0±0.1	0.075
DEP_pH 2_PS	0.0057	0.999	-1.39±0.13	0.995	-41.8±2.4	0.998	25.7±2.6	0.066
DEP_pH 7_PS	0.0025	0.973	-1.57±0.18	0.993	-28.3±3.3	0.993	14.9±3.0	0.112
DEP_pH 7_UV/H_2O_2	0.0541	0.993	-2.30±0.42	0.990	-6.8±1.3	0.989	2.4±0.2	0.101
DBP_pH 2_PS	0.015	0.995	-0.73±0.10	0.983	-31.0±2.0	0.997	39.0±3.4	0.080
DBP_pH 7_PS	0.0039	0.987	-0.63±0.07	0.989	-24.6±1.8	0.996	35.3±4.5	0.136
DBP_pH 7_UV/H_2O_2	0.1115	0.985	-0.92±0.16	0.974	-9.3±2.0	0.960	9.0±2.3	0.093
DEP_pH 7_TBA PS	0.0007	0.970	-1.35±0.12	0.996	-39.8±5.7	0.989	24.1±4.3	0.478
DEP_pH 2_TBA PS	0.0007	0.965	-1.07±0.29	0.989	-38.8±7.7	0.988	30.5±2.2	0.606

618a. Uncertainty given as 95% confidence interval.

619

620 **Table 2.** Carbon and hydrogen AKIEs of DEP for investigated experimental systems.

Conditions	Dominant radical	ε_C (‰)	^{13}C- AKIE	ε_H (‰)	^{2}H- AKIE
UV/H_2O_2 at pH 7	HO· radical	-2.30±0.42	1.028	-6.8±1.3	1.11
TBA quench at pH 2	$SO_4^{\cdot-}$ radical	-1.07±0.29	1.013	-38.8±7.7	2.19
TBA quench at pH 7	$SO_4^{\cdot-}$ radical	-1.35±0.12	1.016	-39.8±5.7	2.26
PS oxidation at pH 2	$SO_4^{\cdot-}$ radical	-1.39±0.13	1.017	-41.8±2.4	2.41
PS oxidation at pH 7	$SO_4^{\cdot-}$ + HO·	-1.57±0.18	n.d.[a]	-28.3±3.3	n.d.[a]

621 a. n.d.: not determined.

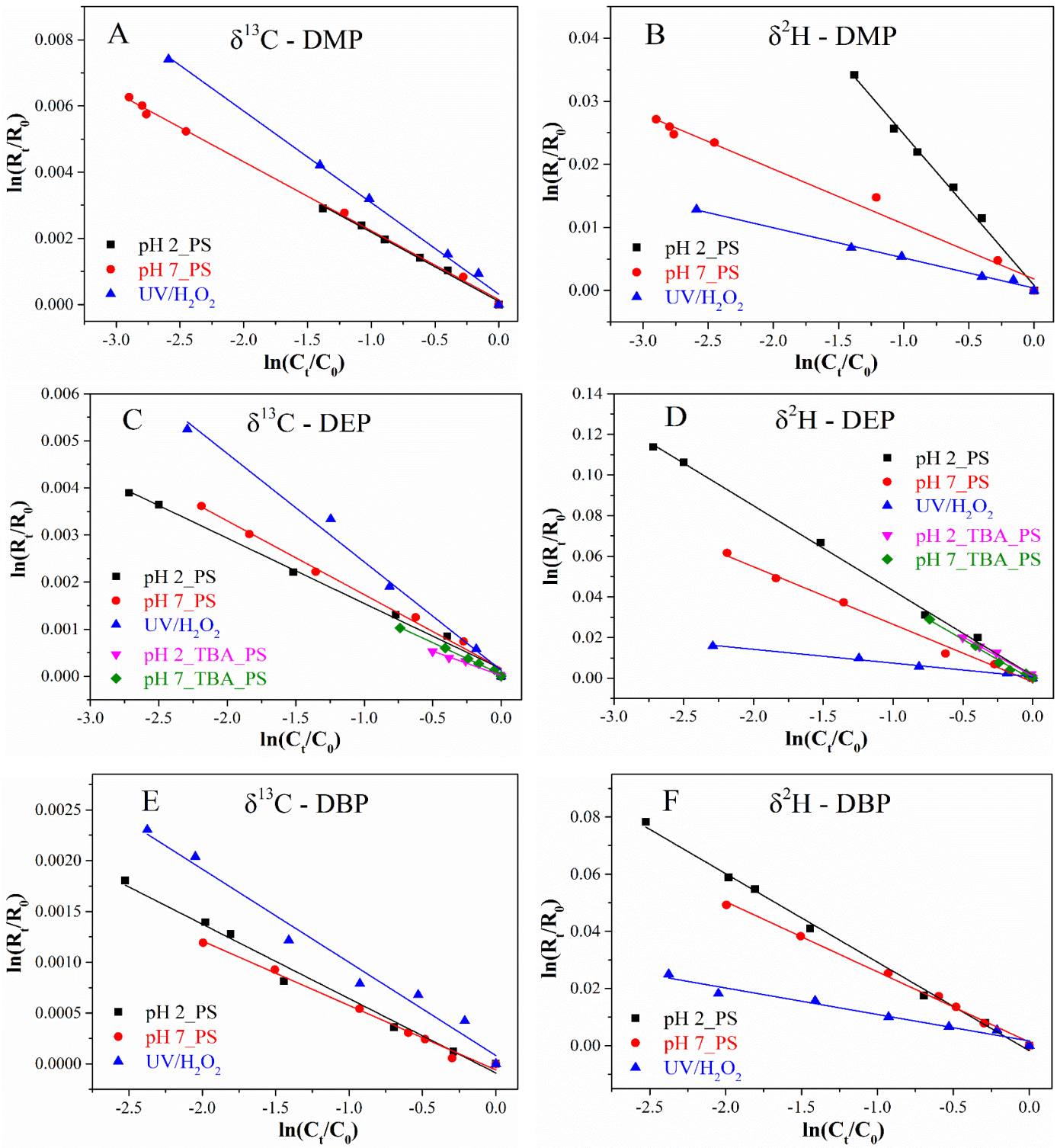

622**Fig. 1.** Rayleigh regression of carbon (left panels, A, C, E) and hydrogen (right panels, B, D, F)

623isotope data during chemical oxidation reactions of PAEs (DMP, DEP and DBP).

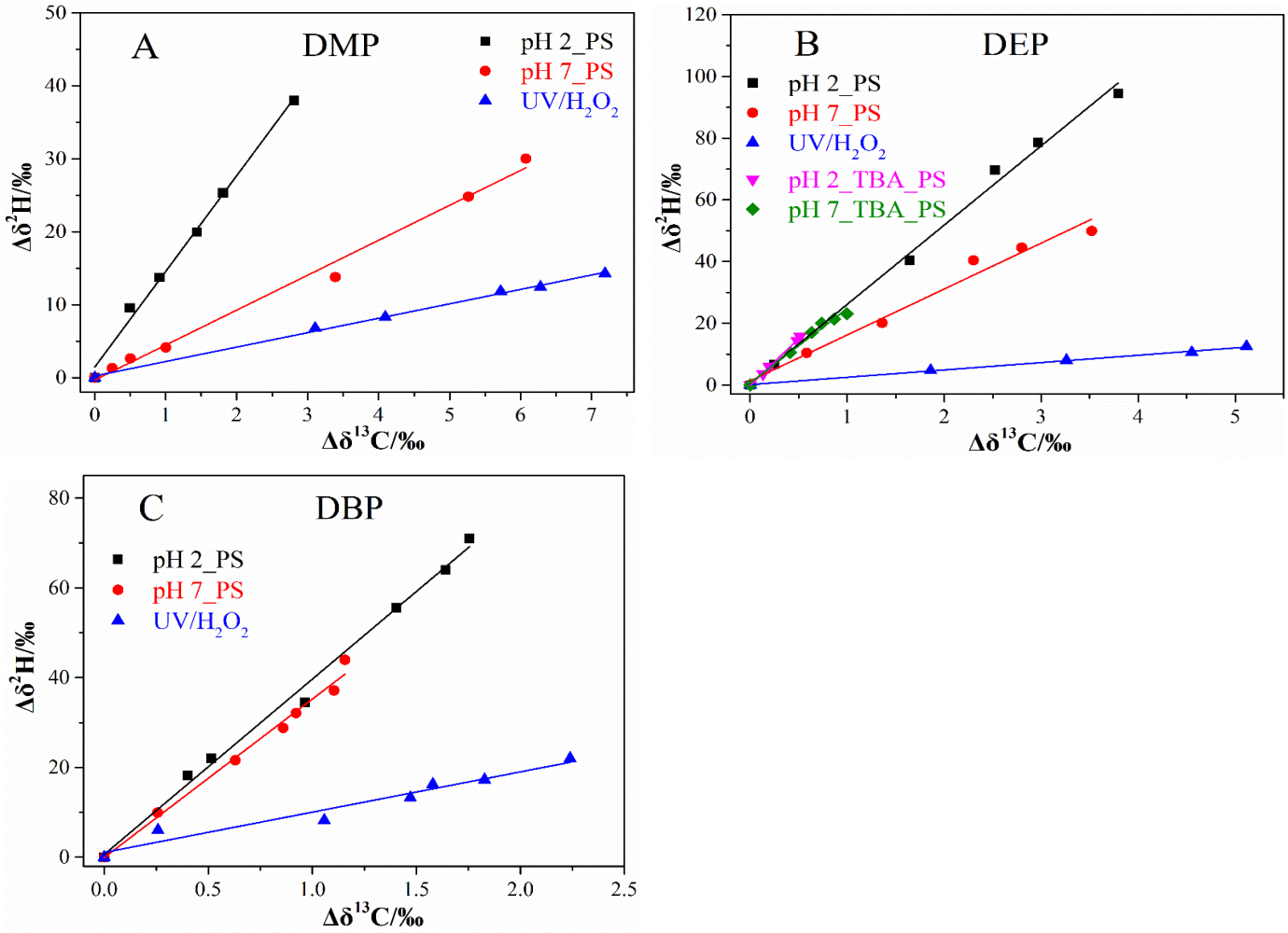

Fig. 2. Correlation of ^{2}H and ^{13}C isotope fractionation for DMP (A), DEP (B) and DBP (C) during chemical oxidation reactions.

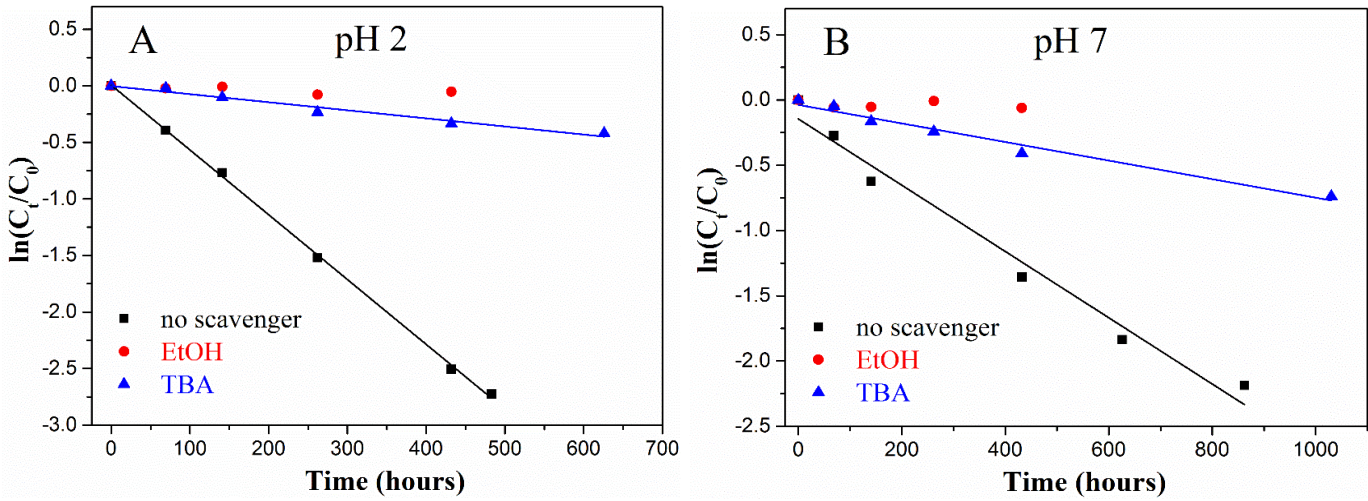

626**Fig. 3.** Degradation kinetic curves of DEP during the study of radical quenching at pH = 2 (A) and

627pH = 7 (B).